

Predicting Succinylation Sites in Proteins with Improved Deep Learning Architecture

Olusola T. Odeyomi and Gergely Zaruba

Department of Electrical Engineering and Computer Science

Wichita State University

Wichita, Kansas 67260-0083

Email: otodeyomi@shockers.wichita.edu

gergely.zaruba @wichita.edu

Abstract—Post-translational modifications (PTMs) in proteins occur after the process of translation. PTMs account for many cellular processes such as deoxyribonucleic acid (DNA) repair, cell signaling and cell death. One of the recent PTMs is succinylation. Succinylation modifies lysine residue from -1 to $+1$. Locating succinylation sites using experimental methods, such as mass spectrometry is very laborious. Hence, computational methods are favored using machine learning techniques. This paper proposes a deep learning architecture to predict succinylation sites. The performance of the proposed architecture is compared to the state-of-the-art deep learning architecture and other traditional machine learning techniques for succinylation. It is shown from the performance metrics that the proposed architecture provides a good trade-off between speed of computation and classification accuracy.

I. INTRODUCTION

Post-translational modification (PTMs) occur in proteins by the addition of a covalent bond after protein is synthesized from messenger RNA (mRNA) by ribosomes. PTMs are very important in many cellular processes such as DNA repair, cell death and cell signaling. Sites in protein that undergo PTMs are those that can act as a nucleophile in reactions. There are many types of PTMs such as phosphorylation, glycosylation, succinylation etc. Protein succinylation is a recently emerged protein post-translational modification on lysine. Succinylation introduces a large structural moiety (e.g., 100 Da) and it modifies the net charge of modified lysine residue from -1 to $+1$. It is suggested that protein succinylation is important in cellular metabolism and many other cellular functions. Experimental methods for determining protein succinylation sites, such as mass spectrometry, are laborious and not cost-effective. Computational methods are thus favored.

Most existing work that uses computational methods employs machine learning techniques such as in iSuc-PseAAC [1], iSuc-PseOPT [2], pSuc-Lys [3], SuccinSite [4], SuccinSite 2.0 [5], GPSuc [6], and PSucE [7]. The problem with traditional machine learning methods is the requirement for manual extraction of features. Also, traditional machine learning methods cannot handle very large FASTA file reliably. Most deep learning methods in literature are applied to phosphorylation rather than succinylation, and use one-hot encoding that does not account for the proper classification of features. However,

there is a recent work that uses a deep learning architecture for succinylation with state-of-the-art performance. The authors called this architecture deepSuccinylSite-embedding [8].

Thus, in this paper, the performance of deepSuccinylSite-embedding is compared with the performance of a proposed deep learning architecture called DeepSuccinylCNN+LSTM. While deepSuccinylSite uses 2D convolutional network, the novel architecture uses 1D Convolutional network + LSTM (Long Short-Term Memory). The motivation for this architecture is comparable performance with deepSuccinylSite but with faster computational speed. This is very important when dealing with large FASTA file.

II. DATASET PREPROCESSING

The dataset for this computation was obtained from experimentally derived lysine residue reported in [6] and [7]. Proteins with more than thirty percent 30% sequence identity were removed using CD-HIT. This left a remainder of 5009 succinylation sites, and 53,542 non-succinylation sites. Out of these, 4755 succinylation sites and 50,565 non-succinylation sites were used as training set. This meant that 254 succinylation sites and 2977 non-succinylation sites were used as independent test set. However, 5 out of the 4755 positive sites were lost because they contained other characters. The datasets were balanced using undersampling. The final training set had 4750 positive and 4750 negative sites. The final independent test set contained 254 positive and 254 negative sites. The optimal window size was 33. If left and right side were less than half the size of the window, then a pseudo-residue “-” was used to recover all positive sites. Table 1 shows the size of the positive and negative sites for the training and independent test sets.

III. INPUT MODELING

The novel deep learning architecture Conv1D+LSTM used keras embedding layer similar to DeepSuccinylSite. The embedding layer came before the first convolutional layer. The embedding layer output was a 21-dimensional vector space. The embedding layer grouped co-occurring items together. Other types of sophisticated embedding techniques common in natural language processing could be used, such as Word2Vec

TABLE I
SIZE OF TRAINING AND INDEPENDENT TEST SET

Dataset	Positive	Negative
Training	4750	4750
Independent Test	254	254

or GloVe, but they often come with increased cost of computation. The training set was divided into 80% training and 20% validation set. Validation was done at every epoch to prevent overfitting. Checkpointer was used to select the optimal model from the epochs based on validation accuracy. The protein sequence dataset was in FASTA format. The input dimension to the convolutional neural network had a dimension of 33 by 21, since the window size was 33, and the vector size of the output from the embedding size was 21. An advantage of using deep learning is the elimination of handcrafted features, which is often laborious.

IV. DEEP LEARNING ARCHITECTURE

The input to the first layer of the deep learning architecture is the embedding layer. DeepSuccinylSite used a Lambda layer after this embedding layer, but the Lambda layer was not included in the architecture used in this paper. Three convolutional layers were used with 64, 128 and 256 number of neurons respectively. The hidden layers were for hierarchical feature extraction. Although, DeepSuccinylSite used 2D convolutional layers instead of 1D convolutional layers for more feature extraction, it was observed that it slowed down the speed of the computation in comparison to the improvement obtained. Hence, 1D convolutional layer was used together with LSTM in DeepSuccinylCNN+LSTM. The kernel size used was 17, since the PTM site lied in the 17th position. The use of this kernel size removed the need for padding. Dropouts of 0.6 were inserted between the convolutional layers to avoid overfitting. The activation function was linear rectifier (ReLU) because it could minimize overfitting and maximize the predictive power of the model. A single maxpool layer was used followed by the LSTM layer. Three dense layers with neurons size 256, 768 and 1024 were used. Dropouts of 0.5, 0.5 and 0.25 were used between the dense layers respectively. The optimization used was Adam optimization, which is an adaptive stochastic gradient optimization algorithm. Adam optimization inherently possesses the advantages of adaptive gradient optimization and root-mean-square propagation. Also, binary cross entropy was used as the loss function because this is a binary classification problem. The final output layer contained 2 nodes and used softmax activation function. Figure 1 is a snapshot of the parameters for the simulation.

V. RESULTS

For this simulation, 10-fold cross validation was used. This means that the training set was divided into 9 parts for training and 1 part for validation at every epoch. This process is repeated, so that each part is used as the validation set. The

Layer (type)	Output Shape	Param #
embedding_8 (Embedding)	(None, 33, 21)	5376
conv1d_16 (Conv1D)	(None, 33, 64)	22912
dropout_28 (Dropout)	(None, 33, 64)	0
conv1d_17 (Conv1D)	(None, 33, 128)	139392
dropout_29 (Dropout)	(None, 33, 128)	0
conv1d_18 (Conv1D)	(None, 33, 256)	557312
dropout_30 (Dropout)	(None, 33, 256)	0
max_pooling1d_6 (MaxPooling1d)	(None, 16, 256)	0
lstm_5 (LSTM)	(None, 300)	668400
dense_17 (Dense)	(None, 1024)	308224
dropout_31 (Dropout)	(None, 1024)	0
dense_18 (Dense)	(None, 768)	787200
dropout_32 (Dropout)	(None, 768)	0
dense_19 (Dense)	(None, 256)	196864
dropout_33 (Dropout)	(None, 256)	0
dense_20 (Dense)	(None, 2)	514
Total params: 2,686,194		
Trainable params: 2,686,194		
Non-trainable params: 0		

Fig. 1. A snapshot of the parameters for DeepSuccinylCNN+LSTM architecture

performance metrics for the simulation are Matthew correlation, specificity and sensitivity. These performance metrics are defined below.

A. Sensitivity

Sensitivity is a measure of how many positive succinylation sites were correctly identified. It is given by the (3) below:

$$sensitivity = \frac{TP}{TP + FN} \quad (1)$$

where TP refers to the True Positives and FN refers to the False Negatives.

B. Specificity

Specificity measures the number of negative succinylation sites correctly identified.

$$specificity = \frac{TN}{TN + FP} \quad (2)$$

where TN refers to the True Negatives and FP refers to the False Positives. The TP , TN , FP and FN were gotten from the confusion matrix.

C. Matthew Correlation Coefficient

The Matthew correlation coefficient (MCC) is a measure of the correlation between the predicted binary class and the observed binary class. It ranges from -1 to $+1$. A coefficient

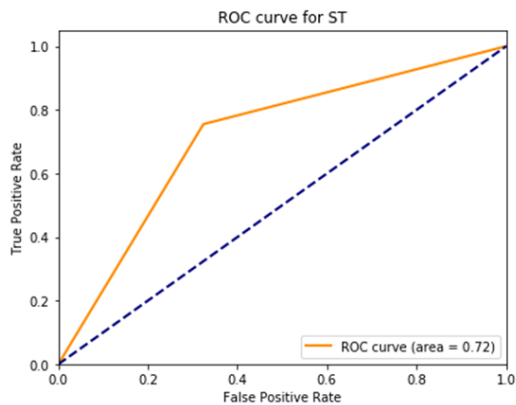


Fig. 2. ROC curve for DeepSuccinylSite.

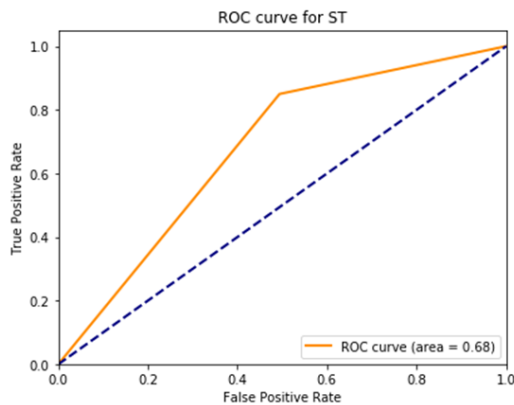


Fig. 3. ROC curve for DeepSuccinylCNN+LSTM.

of -1 means that there is a total disagreement between the predicted and the observed binary classifications. A coefficient of 0 means that the prediction is random. A coefficient of 1 means that there is a perfect agreement between the predicted and the observed binary classifications. The formula for MCC is given as

$$MCC = \frac{(TP \times TN) - (FP \times FN)}{\sqrt{(TP + FP)(TP + FN)(TN + FP)(TN + FN)}} \quad (3)$$

D. Receiver Operating Characteristics Curve

The receiver operating characteristic curve (ROC) is a graphical tool to investigate the discriminatory ability of a binary classifier. It compares sensitivity to specificity, with the true positive rate on the y-axis, and the false positive rate on the x-axis. The diagonal line in the plot divides the ROC space. Points above this diagonal line depicts good classification results, while points below this line depicts poor classification results.

E. Area Under ROC Curve

The area under the ROC curve (AUC) measures the entire area under the ROC curve. It can be defined as the probability that a binary classifier will rank higher a randomly chosen positive site than a randomly chosen negative site. A classifier whose predictions are completely wrong has an AUC of 0.0 , while a classifier whose predictions are completely correct has an AUC of 1.0 . Thus, the AUC ranges from 0 to 1 .

The simulation used the same datasets, window size and embedding size to compare the performance of the state-of-the-art DeepSuccinylSite deep learning architecture and the proposed deep learning architecture. Both deep learning architectures were trained on the training set, but their performance were measured on the independent test set. The performance of both deep learning architectures is shown in Table II.

The ROC curves for DeepSuccinylSite and DeepSuccinylCNN+LSTM are both shown in Figs. 2 and 3 respectively. It can be observed from Table II that DeepSuccinylSite has a

higher MCC and specificity than DeepSuccinylCNN+LSTM, but a lower sensitivity. However, the difference is not much. Also, from Figs. 2 and 3, it can also be observed that DeepSuccinylSite has a higher AUC than DeepSuccinylCNN+LSTM. The main advantage of DeepSuccinylCNN+LSTM over DeepSuccinylSite is faster computation. The average time for running an epoch in DeepSuccinylSite was 29 seconds. The average time for running an epoch in DeepSuccinylLSTM+CNN was 20 seconds. However, the number of epoch used was 60 and the batch size is 256. This meant that for 60 epochs, the average running time difference was 540 seconds, and for 256 batch size, the average running time difference was 38.4 hours, using the same computing resource, i.e., a Intel core i7 HP computer. Although, this running time difference will be reduced by using a graphics processing unit (GPU). However, when the size of the datasets increase, the running time difference will become obvious.

There are other traditional machine learning methods for predicting succinylation sites that utilizes other features apart from the amino-acid sequence. Such features include the physiochemical properties such as the Pseudo Amino Acid Composition (PAAC), K-spaced Amino Acid Pairs (AAP) etc. These machine learning methods are iSuc-PseAAC [1], iSuc-PseOpt [2], PSuc-Lys [3], SuccinSite [4], SuccinSite2.0 [5] GPSuc[6] and PSucE [7]. Table III shows that the performance of these machine learning methods in comparison with DeepSuccinylLSTM+CNN. The values for sensitivity, specificity and MCC for the machine learning methods were obtained directly from the published articles. It can be seen from Table III that DeepSuccinylCNN+LSTM still performs better than these machine learning methods. Hence, DeepSuccinylCNN+LSTM provides a good trade-off between speed of computation and performance.

VI. BRIEF OVERVIEW OF CONVOLUTIONAL NEURAL NETWORKS

Convolutional neural network (CNN) was inspired by the biological processes in the visual cortex of a rabbit. Unlike multi-layer perceptron which is fully connected, the CNN

TABLE II
DEEPSUCCINYLSITE VERSUS DEEPSUCCINYLCNN+LSTM

Prediction Schemes	Sensitivity	Specificity	MCC
DeepSuccinylSite	0.73	0.70	0.43
DeepSuccinylSiteCNN+LSTM	0.77	0.63	0.39

TABLE III
TRADITIONAL MACHINE LEARNING VERSUS DEEPSUCCINYLCNN+LSTM

Prediction Schemes	Sensitivity	Specificity	MCC
iSuc-PseAAC	0.12	0.89	0.01
iSuc-PseOpt	0.30	0.70	0.04
Psuc-Lys	0.22	0.83	0.04
SuccinSite	0.37	0.88	0.20
SuccinSite2.0	0.45	0.88	0.26
GPSuc	0.50	0.88	0.30
PSucE	0.38	0.89	0.20
DeepSuccinylSiteCNN+LSTM	0.77	0.63	0.39

reduces the number of training parameters by sharing weights. CNN has been successfully for image classification [9]. It has been successful for automatically extracting features without the need for human intervention unlike traditional machine learning techniques. However, it still has the challenge of pose estimation in 3D images.

CNN consists of an input layer, at least one hidden layer, and an output layer. The input layer interfaces with the object. The hidden layers is necessary for feature engineering. The hidden layers comprises the convolutional layer, where a sliding-dot product operation occurs, the ReLu layer as the activation function, the pooling layer for downsampling and feature extraction, and the fully connected dense layer that identifies the object. The output layer does the classification using the softmax function.

VII. BRIEF OVERVIEW OF LONG SHORT TERM MEMORY

Long Short Term Memory (LSTM) is a type of Recurrent Neural Network (RNN) deep learning architecture useful for processing sequential data such as speech and text [10]. Also, it is useful for processing time-series data. Unlike CNN which is a feedforward architecture, LSTM possesses feedback architecture.

LSTM consists of a cell, an input gate, and a forget gate. The cell remembers values over arbitrary time intervals, while the three gates control the flow of information in and out of the cell. One advantage of LSTM over traditional RNN is that it overcomes the challenge of vanishing gradient encountered in traditional RNNs. The activation function for LSTM is commonly the sigmoid function.

VIII. CONCLUSION AND FUTURE WORK

Succinylation is a post-translational modification process in proteins that plays an important role in many cellular functions. Finding the succinylation sites using experimental methods such as mass spectrometry is very laborious. Hence, computational methods are favored. Therefore, this paper used an improved deep learning architecture called DeepSuccinylCNN+LSTM to predict positive succinylation

sites. First, the performance of DeepSuccinylSiteCNN+LSTM was compared with DeepSuccinylSite, the state-of-the-art deep learning architecture for succinylation. It was shown that DeepSuccinylCNN+LSTM performed close to DeepSuccinylSite, but with a better trade-off in terms of computational speed. Second, the performance of DeepSuccinylCNN+LSTM was compared with other traditional machine learning architectures for succinylation in literature. It was shown that DeepSuccinylCNN+LSTM performed better using some well-known performance metrics. Hence, it can be concluded that DeepSuccinylCNN+LSTM is better favored when large datasize is used, judging by its computational speed and performance accuracy.

This work can be extended to finding better deep learning architecture that will have the best performance in terms of speed and other performance metrics. More so, novel embedding technique may be used for better performance.

REFERENCES

- [1] Y. Xu, Y.-X. Ding, J. Ding, Y.-H. Lei, L.-Y. Wu, and N.-Y. Deng, "isuc-pseaac: predicting lysine succinylation in proteins by incorporating peptide position-specific propensity," *Scientific reports*, vol. 5, p. 10184, 2015.
- [2] J. Jia, Z. Liu, X. Xiao, B. Liu, and K.-C. Chou, "isuc-pseopt: identifying lysine succinylation sites in proteins by incorporating sequence-coupling effects into pseudo components and optimizing imbalanced training dataset," *Analytical biochemistry*, vol. 497, pp. 48–56, 2016.
- [3] —, "psuc-lys: predict lysine succinylation sites in proteins with pseaac and ensemble random forest approach," *Journal of theoretical biology*, vol. 394, pp. 223–230, 2016.
- [4] M. M. Hasan, S. Yang, Y. Zhou, and M. N. H. Mollah, "Succinsite: a computational tool for the prediction of protein succinylation sites by exploiting the amino acid patterns and properties," *Molecular bioSystems*, vol. 12, no. 3, pp. 786–795, 2016.
- [5] M. M. Hasan, M. S. Khatun, M. N. H. Mollah, C. Yong, and D. Guo, "A systematic identification of

- species-specific protein succinylation sites using joint element features information,” *International journal of nanomedicine*, vol. 12, p. 6303, 2017.
- [6] M. M. Hasan and H. Kurata, “Gpsuc: Global prediction of generic and species-specific succinylation sites by aggregating multiple sequence features,” *PloS one*, vol. 13, no. 10, p. e0200283, 2018.
- [7] Q. Ning, X. Zhao, L. Bao, Z. Ma, and X. Zhao, “Detecting succinylation sites from protein sequences using ensemble support vector machine,” *BMC bioinformatics*, vol. 19, no. 1, p. 237, 2018.
- [8] N. Thapa, M. Chaudhari, S. McManus, K. Roy, R. H. Newman, H. Saigo, and D. B. Kc, “Deepsuccinylsite: a deep learning based approach for protein succinylation site prediction,” *BMC bioinformatics*, vol. 21, pp. 1–10, 2020.
- [9] A. Krizhevsky, I. Sutskever, and G. E. Hinton, “Imagenet classification with deep convolutional neural networks,” in *Advances in neural information processing systems*, 2012, pp. 1097–1105.
- [10] S. Hochreiter and J. Schmidhuber, “Long short-term memory,” *Neural computation*, vol. 9, no. 8, pp. 1735–1780, 1997.